J. Membrane Biol. 114, 37–52 (1990)

The Journal of
Membrane Biology

Characterization of a 25-pS Nonselective Cation Channel in a Cultured Secretory Epithelial Cell Line

D.I. Cook, P. Poronnik, and J.A. Young
Department of Physiology, University of Sydney, NSW 2006 Australia

Summary. We have studied a 25-pS nonselective cation channel from the apical membranes of cell line ST_{885}, derived from neonatal mouse mandibular glands. Its Cl^- permeability was not significantly different from zero. The permeabilities (relative to Na^+) for inorganic cations were NH_4^+ (1.87) > K^+ (1.12) > Li^+ (1.02) > Na^+ (1) > Rb^+ (0.81) > Mg^{2+} (0.07) > Ca^{2+} (0.002), and for organic cations, guanidinium (1.61) > ethanolamine (0.70) > 4-aminopyridine (0.66) > diethylamine (0.54) > piperazine (0.25) > Tris (0.18) > N-methylglucamine (0.12). The Tris and N-methylglucamine permeabilities differed significantly from zero. Fitting the Renkin equation indicated that the channel had an equivalent pore radius of 0.49 nm. The channel was activated by Ca^{2+} on the cytosolic surface (>0.1 mmol/liter) with a Hill coefficient of 1.2; it was also activated by depolarization. Open- and closed-time histograms indicated that it had at least two open and two closed states. The channel was blocked by cytosolic AMP or ATP (0.1 mmol/liter). It was also blocked by the Cl^- channel blocker, diphenylamine-2-carboxylate (DPC; 0.1 mmol/liter), applied to the extracellular but not the cytosolic surface. 4-Aminopyridine, which permeated the channel when applied to the extracellular surface, blocked it when applied in low concentrations (5 mmol/liter) to the cytosolic surface. Quinine (0.1 mmol/liter) blocked from both the extracellular and cytosolic surfaces, blockade from either side being enhanced by depolarization. The channel was held open by application of SITS (0.1 mmol/liter) to the cytosolic surface. The channel shows striking similarities to the nicotinic acetylcholine receptor channel, *viz.*, both channel types are abnormally permeable to 4-aminopyridine applied externally, and their selectivity sequences for inorganic ions are similar and for organic cations are identical.

Key Words nonselective cation channel · ACh receptor channel · epithelia · organic and inorganic cation permeation · channel pore size · Renkin equation

Introduction

Ca^{2+}-activated nonselective cation channels were first reported in 1981 in cultured rat ventricular myocytes [6]. Since then, cation channels that have a single-channel conductance in the range 15–40 pS, that discriminate poorly between Na^+ and K^+, and are activated by Ca^{2+} from the cytosolic surface, have been observed in a wide variety of tissues: neuroblastoma cells [39], rat and mouse pancreatic acinar cells [11, 19, 21], rat and mouse salivary endpiece cells [17], rat lacrimal gland endpiece cells [16], cultured rat Schwann cells [3], rat thyroid follicular cells [18], cultured mouse mandibular endpiece cells [7], human neutrophils [38], cultured rat insulinoma cells [35], cultured rat brown fat cells [33], bursting neurons from *Helix* [24], guinea pig ventricular myocytes [10], rat pancreatic duct cells [12] and guinea pig pancreatic acinar cells [36]. Nevertheless, despite the frequency with which it has been reported, there have been few detailed studies of its properties.

Two features of the channel have led us to study it more closely. (*i*) The first relates to the heterogeneity of its response to Ca^{2+} ions and voltage changes [25]. For example, Sturgess et al. [35] report for insulinoma cells that the channel is activated by Ca^{2+} concentrations greater than 10^{-4} mol/liter and by depolarization of the cell membrane potential, whereas, in mouse pancreatic acinar cells, it is activated by Ca^{2+} concentrations as low as 5×10^{-7} mol/liter and is not sensitive to changes in transmembrane potential [19, 21]. (*ii*) The second feature concerns the function of the channel in epithelial cells, particularly cells secreting salt and water. Thus, although the Ca^{2+}-activated nonselective cation channel has been found in many epithelia, and, in at least one case, cell-attached patch studies have shown that it can be activated by a secretomotor agonist [20], there is currently no satisfactory explanation of its role in secretion. The problem is that, when active, it will permit the entry of Na^+ into the cell and thereby reduce the Na^+ gradient across the basolateral membrane, which would be expected to impair the efficiency of any secretory mechanism based on an intraepithelial current loop driven by Na^+-coupled Cl^- cotransport with development of an intraepithelial current loop [8, 27, 34,

40]. This will occur whether it is in the basolateral membrane, as in mouse pancreatic acinar cells [19], or in the apical membrane, as in rat pancreatic duct cells [12]. It has been suggested that the nonselective cation channel provides a pathway by which Ca^{2+} enters the cytosol from the extracellular medium following secretomotor stimulation [26] although convincing evidence of this is so far lacking. An alternative role was proposed by Marty et al. [16] who suggested that sustained exocrine secretion is not based on a current loop but, rather, is driven by the movement of K^+ across the apical membrane. In this scheme, the role of the nonselective channel in the basolateral membrane would be to maintain the supply of Na^+ to the Na^+-, K^+-ATPase so that it continued to pump K^+ into the cell [8].

In the present study we have used a variety of different measurements to characterize the nonselective cation channel in the apical membrane of a cell line derived from mouse mandibular cells (ST_{885}) in which preliminary studies have demonstrated its presence in large numbers [7]. The channel characteristics we have studied include its permeability to a range of inorganic and organic cations, its kinetics, the sensitivity of its open probability to Ca^{2+} and transmembrane potential difference, and its sensitivity to ATP, AMP, quinine, diphenylamine-2-carboxylate and SITS, compounds that have been reported to influence the activity of nonselective cation channels in other tissues [11, 35]. Our most striking finding is that the nonselective cation channel has properties closely resembling those reported for the nicotinic acetylcholine receptor channel.

Materials and Methods

Cell Culture

Cells of the neonatal mouse mandibular cell line, ST_{885} [7], were used between passages 20 and 40. They were maintained in medium 199 supplemented with 10% fetal calf serum at 37°C in an atmosphere of 95% air and 5% CO_2. Some of the experiments were performed on cells grown directly on the bottom of 25-mm plastic petri dishes while others were performed on cells grown on Cytodex® beads [28], but the results were not affected by the choice of culture substratum. Cells were used 1–6 days after plating out, the culture medium being replaced by the control electrolyte solution immediately before the start of the experiment.

Patch-Clamp Methods

Isolated membrane patches, in either the inside-out or the outside-out configuration [13], were used in all experiments. Patch-clamp pipettes, pulled from borosilicate microhematocrit tubes (Modulohm, Denmark), had resistances of 10–15 MΩ when filled with the control solution. The pipette bubble number [22] was approximately 6, which corresponds to a tip diameter of approximately 0.3 μm [15]. The bath electrode was a Ag/AgCl pellet (Clark Electromedical, Reading, England) which was placed directly in the bath solution except in experiments in which the bath solution Cl^- was altered, in which case the Ag/AgCl electrode was connected to the bath via an agar bridge filled with the control NaCl bath solution.

An EPC-7 extracellular patch-clamp amplifier (List Electronik, Darmstadt, FRG) was used to measure single-channel currents which were then recorded on tape with a video cassette recorder and a Sony 501-ES PCM unit modified as described by Bezanilla [4]. Currents were replayed, filtered at 500 Hz with an 8-pole Bessel filter, and digitized at 1 kHz with a 12-bit AD converter before being analyzed on a PDP micro-11/73 computer. Tracings for illustrative purposes were printed out by the computer on a laser printer. Single-channel currents, open-state probabilities, and open- and closed-time distributions were determined with the aid of an analysis program based on an algorithm published by Sachs, Neil and Barkakati [31]. In the present paper, outward current, defined as current leaving the pipette, has been indicated as an upward deflection in all traces, and potential differences have been defined relative to the bath potential. Experiments were performed at 20°C.

Statistical Methods

All results are presented as means ± SEM. The reversal potentials were estimated by fitting the appropriate form of the generalized Goldman equation to the experimental current-voltage relations. The use of this method is justified by the extremely good fit that the Goldman equation gives to the experimental current-voltage data. The statistical tests employed were general tests based on linear models [23] relying on the F statistic. For example, to test whether a channel had a significant permeability to Cl^-, the current-voltage relation was fitted first by the Goldman equation using a least-squares method on the assumption that the channel was permeable to both Na^+ and Cl^-, and the residual sum of squares ($SSQ_{(P_{Cl}\neq 0)}$) was noted. Then the data were again fitted with the Goldman equation, this time on the assumption that only $Na^+$was permeant, and the new residual sum of squares ($SSQ_{(P_{Cl}=0)}$) was found. The test statistic, F, to determine whether P_{Cl} differs significantly from zero can then be calculated from the following equation:

$$F = \frac{SSQ_{(P_{Cl}=0)} - SSQ_{(P_{Cl}\neq 0)}}{SSQ_{(P_{Cl}=0)}} \times (n - p) \quad (1)$$

where n is the number of data and p is the number of parameters in the model; in this case $p = 2$. In this simple example, the method gives the same results as a t test but it can readily be generalized to test simultaneously whether a channel is permeable to several ions. For instance, we may test simultaneously whether a channel is permeable to Na^+, Cl^- and SO_4^{2-} whereas the t test cannot be used in these circumstances.

In this paper, we require confidence limits for the ratio P_x/P_{Na}, where the subscript x denotes any ion. Linear least-squares fits of the appropriate form of the Goldman equation will give estimates of P_x and P_{Na}, together with their respective variances and covariances, and these estimates can then be used to calculate confidence limits for P_x/P_{Na} by use of the Bonferroni joint

confidence interval for P_x and P_{Na}, as given by the following rectangle [23]:

$$P'_x - B \cdot s'_x \leq P_x \leq P'_x + B \cdot s'_x \quad (2a)$$

$$P'_{Na} - B \cdot s'_{Na} \leq P_{Na} \leq P'_{Na} + B \cdot s'_{Na} \quad (2b)$$

where P'_{Na} and P'_x are the least-squares estimates of P_{Na} and P_x and s'_{Na}, s'_x are the standard errors of those estimates and the constant, B, is defined as

$$B = t(1 - \frac{\alpha}{4}; n - 2) \quad (3)$$

when t is Student's t distribution and $(1 - \alpha)$ is the confidence coefficient. The confidence limits of the ratio P_x/P_{Na} are given by the ratio of the co-ordinates of two of the corners of the Bonferroni confidence limits. If the confidence limits of P_x lie entirely in the positive range, then the confidence limits of the ratio are:

$$\frac{P'_x - B \cdot s'_x}{P'_{Na} + B \cdot s'_{Na}} \leq \frac{P_x}{P_{Na}} \leq \frac{P'_x + B \cdot s'_x}{P'_{Na} - B \cdot s'_{Na}} \quad (4)$$

and, if the confidence limits of P_x include 0, the confidence limits of the ratio are:

$$\frac{P'_x - B \cdot s'_x}{P'_{Na} - B \cdot s'_{Na}} \leq \frac{P_x}{P_{Na}} \leq \frac{P'_x + B \cdot s'_x}{P'_{Na} - B \cdot s'_{Na}}. \quad (5)$$

A problem posed by our data concerns our ability to be certain that there is only one channel active in a given patch. Although most of the patches we obtained contained two or more active channels, in order to perform a kinetic analysis we had to select only those in which one active channel was present. Since we had to use the failure to observe multiple openings as our criterion for recognizing such a patch, the question arose of how confident in a given case we could be that there was really only one active channel present. It can readily be shown that, for a patch in which there are N channels present with simple two-state kinetics, the probability, P, of p openings occurring without multiple openings being observed is:

$$P = \left(\frac{n}{N(1 + t_o/t_c) - t_o/t_c}\right)^p \quad (6)$$

where t_o and t_c are the experimentally determined mean open and closed times. This equation is similar to that proposed by Colquhoun and Hawkes [5], except that it is not subject to their restriction of $t_o \ll t_c$. The probability, Π, that a recording showing p single and no multiple openings contains only one active channel is thus:

$$\Pi = \left(\frac{1}{\sum_{N=1}^{N=\infty} (P)}\right) \quad (7)$$

where P is defined in Eq. (6).

Solutions

The composition of the control solution (in mmol/liter) was made up to be: NaCl 145, KCl 5, $CaCl_2$ 2.7, $MgCl_2$ 1.2, NaH_2PO_4 1.2, NaHEPES 7.5, HHEPES 7.5 and glucose 10; the pH was 7.4. This solution was used in both the pipette and the bath except in ion substitution experiments. The composition of the solutions used for the cation substitution experiments are shown in Table 1. In all experiments except those in which Li^+, K^+ or N-methylglucamine was the test cation, we placed the control solution in the bath and the test solution in the pipette. In most experiments the concentration of the test cation was 130 or 150 mmol/liter but, when using Ca^{2-} as the test cation, we could not obtain seals at concentrations greater than 75 mmol/liter. In experiments in which the cation-to-anion selectivity was to be determined, the pipette contained the control solution and the bath solution consisted of the control solution, diluted with 2 parts isotonic sucrose to 1 part control solution. In experiments in which low concentrations of free Ca^{2+} were required, Ca-EGTA buffer was employed: for a free Ca^{2+} concentration of 10^{-9} mol/liter the EGTA concentration was 1.92 mmol/liter and the calcium salt concentration was 0.01 mmol/liter, and for a free Ca^{2+} concentration of 10^{-6} mol/liter, the EGTA concentration was 1.73 mmol/liter and the calcium salt concentration was 1.54 mmol/liter. For the calculation of relative ionic permeabilities from the Goldman equation, ionic activities rather than concentrations were used, the activity coefficients being calculated from the ionic strengths of each solution with the aid of data and methods described in Robinson and Stokes [30]. The activity coefficients we used are given in Table 1. In experiments where the pipette and bath solutions differed at the start of the experiment, a junction potential arose at the pipette tip. This junction potential was determined with an electrometer by measuring the diffusion potential established by the solutions across a dialysis membrane. The pipette potentials were then corrected appropriately. The electrometer was connected to the test solutions with Ag/AgCl pellet electrodes. In no case did the correction exceed 4 mV.

Chemicals

AMP, ATP, 4-acetamido-4′-isothiocyanatostilbene-2,2′-disulphonic acid (SITS), quinine sulphate, HEPES and EGTA were obtained from Sigma (St. Louis, MO). Diphenylamine-2-carboxylate (DPC) was the gift of Professor R. Greger, University of Freiburg, FRG. All other chemicals used were of the highest grade available.

Results

We encountered several channel types in apical membrane patches isolated from the ST_{885} cell line studied in symmetrical solutions of NaCl. The main types observed were a small-conductance Cl^- channel, a 12-pS nonselective cation channel and the nonselective cation channel that is the subject of this paper. We observed this last channel in 68% of 241 excised inside-out patches. In only 10% of the patches in which the channel was observed did it appear (with greater than 99% probability) that only one channel was active, in the majority, two to four channels were simultaneously active and occasionally nine or more channels were seen. SITS, which will be shown below to activate these channels when added to the cytosolic surface of inside-out patches, unmasked up to six channels in patches in

Table 1. Cation concentrations (in mmol/liter) and activity coefficients (γ) of the pipette and bath solutions used in the cation substitution experiments summarized in Tables 2 and 3.[a]

Test cation	Bath solution				Pipette solution			
	Test cation	γ_{test}	Na	γ_{Na}	Test cation	γ_{test}	Na	γ_{Na}
NH_4^+	—	—	153.7[b]	0.76	150	0.74	5	0.76
Rb^+	—	—	153.7[b]	0.76	150	0.74	5	0.76
Guanidinium	—	—	153.7[b]	0.76	150	0.74	5	0.76
Ca^{2+}	2.7	0.58	153.7[b]	0.76	75	0.53	75	0.71
Li^+	120	0.77	31	0.76	—	—	153.7[b]	0.76
K^+	120	0.74	31	0.76	5	0.74	153.7[b]	0.76
N-methylglucamine	120	0.74	31	0.76	—	—	153.7[b]	0.76
Mg^{2+}	1.2	0.59	153.7[b]	0.76	130	0.51	23	0.68
Ethanolamine	—	—	153.7[b]	0.76	130	0.74	23	0.76
Diethylamine	—	—	153.7[b]	0.76	130	0.74	23	0.76
Piperazine	—	—	153.7[b]	0.76	130	0.74	23	0.76
4-Aminopyridine	—	—	153.7[b]	0.76	130	0.74	23	0.76
Tris	—	—	153.7[b]	0.76	130	0.74	23	0.76

[a] Bath and pipette solutions contained (in mmol/liter) Mg^{2+} 1.2, Ca^{2+} 2.7, HEPES buffer 15 and glucose 10; the K^+ concentration varied but was never greater than 5 mmol/liter

[b] The control solution contained (in mmol/liter) Na^+ 153.7, K^+ 5, Mg^{2-} 1.2, Ca^{2+} 2.7, Cl^- 157.8, HPO_4^{2-} 1.2, HEPES 15 and glucose 10.

which only two or three channels has been observed under control conditions.

In a series of eight consecutive cell-attached patches obtained from unstimulated cells, we were able positively to identify the 25-pS channel in four patches, and there were a further two patches in which the 25-pS channel may have been present but we were unable to identify it positively because of the activity of other channel types in the patch. In only two of the eight cell-attached patches could we say that the channel was definitely not active. The activity of the 25-pS channel declined with time after the formation of the cell-attached patch, so that in only one of the four patches in which the channel was initially active did it remain active for more than 20 sec. In two of the four patches in which the 25-pS channel was active, we were able to obtain excised inside-out patches in which the channel remained active. The typical channel activity in a cell-attached patch can be seen in the single-channel recordings in Fig. 1*A*. The current-voltage relation of the nonselective cation channel in cell-attached patches studied under these conditions was linear over the range examined and it indicated a single-channel conductance of 30.5 pS (Fig. 1*A*).

Figure 1*B* shows the typical activity of the nonselective cation channel in an inside-out patch bathed symmetrically in the control NaCl solution. Under these conditions, it was the predominant channel type and although the current-voltage relation appeared to be sigmoidal, the size of the errors were such that the current-voltage relation was found not to be significantly different from a straight line within a range of pipette holding potentials from −80 to +80 mV (Fig. 1*B*). Under these conditions, the single-channel conductance was 25.1 ± 1.0 pS (n = 10), and the reversal potential was +1.2 ± 1.8 mV (n = 10). Dilution of the bath NaCl to 52 mmol/liter with isotonic sucrose shifted the reversal potential to −28.0 ± 3.8 mV (n = 6), and caused the current-voltage relation to rectify (Fig. 2). A linear least-squares fit of the Goldman equation yielded a value for P_{Na} of $4.9 \times 10^{-14} \pm 2.3 \times 10^{-16}$ cm^3 sec^{-1} (n = 3); the value for P_{Cl}, *viz.*, $-2.6 \times 10^{-16} \pm 1.8 \times 10^{-16}$ cm^3 sec^{-1} (n = 3), was not significantly different from zero. The 95% confidence limits for the ratio P_{Cl}/P_{Na}, calculated from Eq. (5) were $-0.005 \leq P_{Cl}/P_{Na} \leq +0.004$. In two experiments we reduced the bathing solution Cl^- to 53 mmol/liter by replacing it with SO_4^{2-}. In these experiments the reversal potentials were found to be −5.3 and +1.3 mV, consistent with our conclusion from the dilution potential measurements that the channel was not appreciably permeable to anions.

The 25-pS channel discriminated very poorly among monovalent inorganic cations, particularly between Na^+ and K^+ (Table 2 and Fig. 2). Thus, in four experiments in which the bathing solution was replaced by one containing 120 mmol/liter K^+ and 31 mmol/liter Na^+, the reversal potential did not

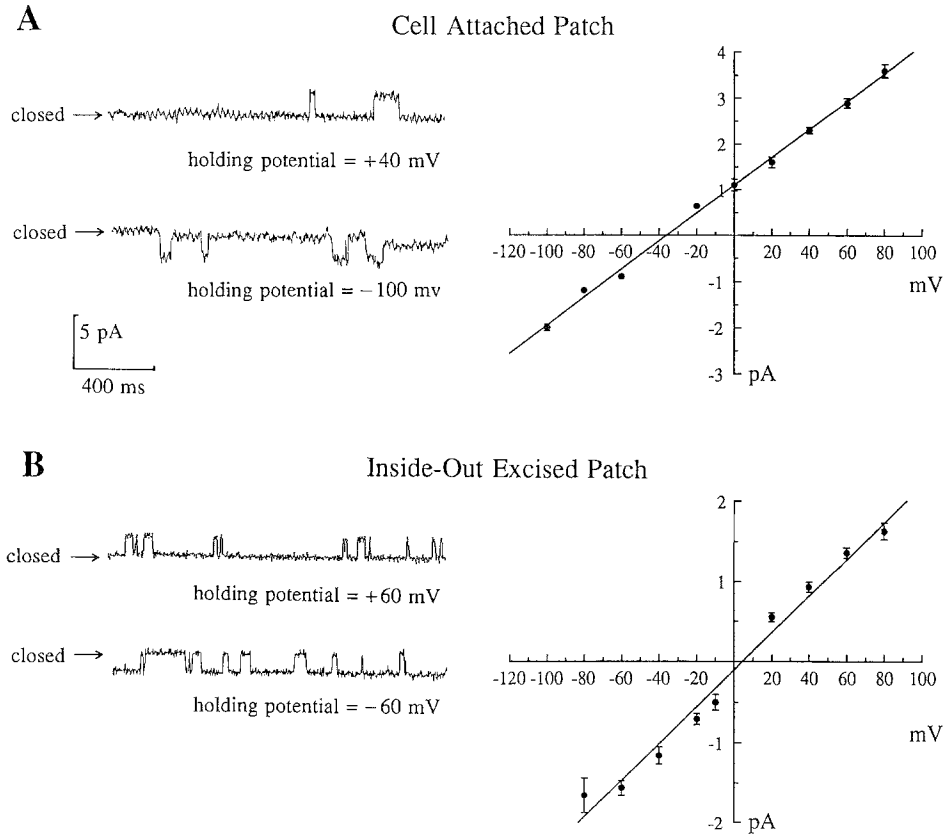

Fig. 1. (*A*) Representative single-channel recordings from a cell-attached patch, together with the current-voltage relation obtained for the nonselective cation channel in cell-attached patches studied under the same experimental conditions, i.e., with the control NaCl solution in the pipette. In these recordings, the nonselective cation channel is responsible for the 2-pA transitions, and the smaller 0.8-pA transitions that are particularly marked in the recording at −100 mV are due to an 8-pS Cl^- channel. The current-voltage relation shown is a least-squares fit and the points shown with error bars are from between three and five experiments. (*B*) Representative single-channel recordings from an excised inside-out patch, together with the current-voltage relation of the nonselective cation channel under the same experimental conditions, i.e., with the control NaCl solution in the pipette. The current-voltage relation shown is a least-squares fit and the points shown with error bars are from between three and 10 experiments. In this and in subsequent figures, currents flowing out of the pipette are defined as positive and are shown as upward deflections. Pipette potentials are defined with respect to the bath

shift significantly and the current-voltage relation remained linear with a slope conductance of 24.7 ± 0.8 pS. The ratio P_K/P_{Na} was estimated to be 1.12 with 95% confidence limits of 1.08 and 1.16. The data in Table 2 and the current-voltage relations shown in Figs. 2 and 3 also show that the channel is highly permeable to NH_4^+, Li^+ and Rb^+, the permeabilities relative to Na^+ being 1.87, 1.02 and 0.81, respectively.

We also investigated the permeability of the channel to the divalent cations, Mg^{2+} and Ca^{2+} (Table 2 and Fig. 2). When the control pipette solution was replaced with 130 mmol/liter Mg^{2+}, 23 mmol/liter Na^+ and 290 mmol/liter Cl^-, the reversal potential shifted to +43.7 ± 1.6 mV (n = 3) (Fig. 2). A linear least-squares fit of the Goldman equation to these data indicated that the channel had a permea-

Table 2. Reversal potential and permeability of the nonselective cation channel in ST_{885} cells to various inorganic ions, expressed relative to the Na^+ permeability.[a]

Ion	Reversal potential (mv)	$\left[\frac{P_x}{P_{Na}}\right]$	95% Confidence limits	n
Li^+	−0.3 ± 1.3	1.02	0.95 –1.09	4
NH_4^+	−10.1 ± 1.6	1.87	1.77 –1.98	3
Na^+	1.2 ± 1.8	1	— —	10
K^+	1.3 ± 1.2	1.12	1.08 –1.16	4
Rb^+	5.0 ± 1.3	0.81	0.79 –0.83	4
Mg^{2+}	43.7 ± 1.6	0.07	0.06 –0.08	3
Ca^{2+}	20.0 ± 0.6	0.002	−0.007–0.010	4
Cl	−28.0 ± 3.8	−0.001	−0.005–0.004	6

[a] The data were obtained from inside-out excised patches.

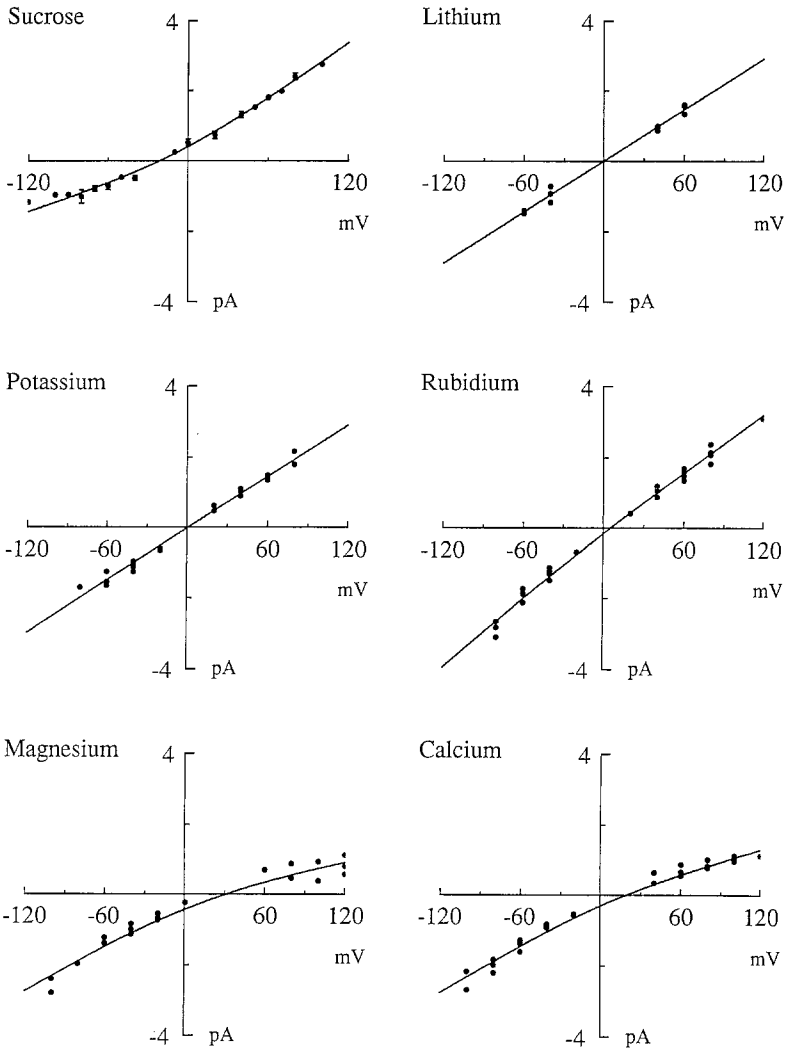

Fig. 2. The current-voltage relations for the experiments summarized in Table 2. The lines are least-squares fits of the Goldman equation, assuming that both Na^+ and the test ion are permeant. The composition of each solution used is as given in Table 1. In the experiments with sucrose, Li^+ and K^+, the bath contained the test solution and the pipette contained the control Na^+-rich solution, whereas in the experiments with Rb^+, Mg^{2+} and Ca^{2+}, the pipette contained the test solution and the bath contained the control solution

bility to Mg^{2+} relative to Na^+ of 0.07. When the pipette contained a solution with 75 mmol/liter $CaCl_2$ and 75 mmol/liter NaCl, the reversal potential shifted to $+20.0 \pm 0.6$ mV ($n = 4$) and the least-squares fit of the Goldman equation showed that Ca^{2+} did not permeate through the channel to any appreciable extent (Fig. 2 and Table 2).

We measured channel permeability relative to Na^+ for a wide range of organic cations with the aim of determining the equivalent pore size of the channel; the current-voltage relations are shown in Fig. 3 and the reversal potentials and the permeability ratios obtained from fitting the Goldman equation to these curves are summarized in Table 3. Both N-methylglucamine and Tris were found to permeate the channel to a small but significant extent. At the other extreme, guanidinium was almost twice as permeant as Na^+. Figure 4 shows a plot of the relative permeability of these cations *vs.* their molecular radii. We found that, with the exception of 4-aminopyridine, they defined a smoothly declining function and when the data were fitted by the Renkin equation (which describes the permeation of a rigid sphere through a cylindrical pore [29]), the equivalent pore radius of the channel was estimated to be 0.49 nm.

We tested the effect of cytosolic free Ca^{2+} in concentrations between 10^{-9} and 10^{-2} mol/liter on channel open probability for inside-out patches while the pipette potential was held at +60 mV. The calcium sensitivity of these channels did not change between 15 sec and 10 min after patch excision. The calcium sensitivity of the channel is shown in Fig. 5. The channel was not active at free Ca^{2+} concentrations of less than 10^{-6} mol/liter, and was half-maximally stimulated at approximately 10^{-3} mol/liter. At the highest Ca^{2+} concentration tested, 10^{-2} mol/liter, the channel was open 67% of the time. A least-squares fit of the Hill equation, *viz.*,

$$P = \left(\frac{P_{max}}{1 + K_d/([Ca^{2+}])^n}\right) \quad (8)$$

Table 3. Reversal potential and permeability of the nonselective cation channel in ST_{885} cells to various organic ions, expressed relative to the Na^+ permeability.[a]

Ion	MW	Reversal potential (mV)	$\left[\frac{P_x}{P_{Na}}\right]$	95% Confidence limits	n
Guanidinium	60.1	−11.7 ± 1.1	1.61	1.53–1.70	3
Ethanolamine	62.1	7.6 ± 1.4	0.70	0.68–0.73	3
Diethylamine	73.1	13.0 ± 2.4	0.54	0.51–0.57	3
Piperazine	87.1	26.4 ± 2.2	0.25	0.23–0.28	3
4-Aminopyridine	95.1	8.6 ± 1.1	0.66	0.61–0.72	3
Tris	121.2	33.1 ± 3.5	0.18	0.16–0.19	4
N-methylglucamine	195.2	−30.8 ± 3.3	0.12	0.08–0.17	4

[a] The data were obtained from inside-out excised patches.

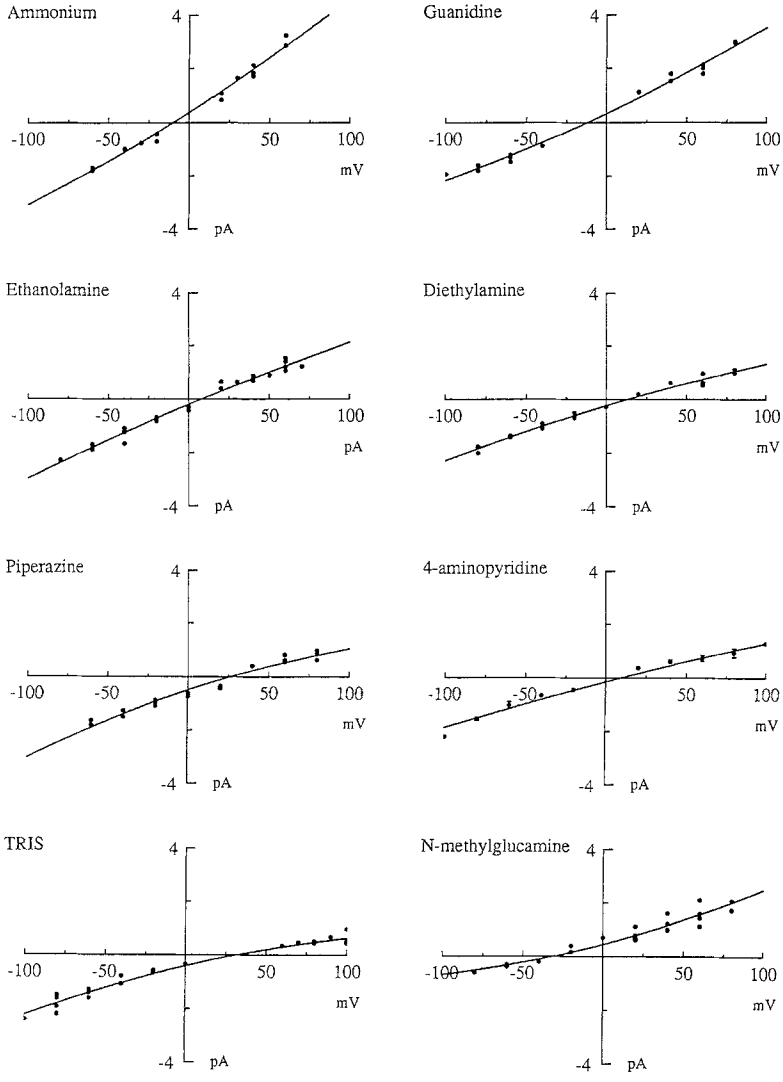

Fig. 3. The current-voltage relations for the experiments summarized in Table 3. The lines are least-squares fits of the Goldman equation, assuming that both Na^+ and the test ion are permeant. The composition of each solution used is as given in Table 1. In the experiments with N-methylglucamine, the bath contained the test solution and the pipette contained the control Na^+-rich solution, whereas in the experiments with the other organic cations, the pipette contained the test solution and the bath contained the control solution

where P is the open probability at any given Ca^{2+} concentration, gave a Hill coefficient (n) of 1.2, with a maximum open probability (P_{max}) of 0.7 and a binding constant (K_d) of 1.8×10^{-3} (mol/liter)^n.

The single-channel tracings (Fig. 1*B*) suggested that the channel was activated by depolarization of the membrane potential. This impression was confirmed by experiments showing the dependence of channel open probability on the holding potential in excised inside-out patches studied with 2.7 mmol/

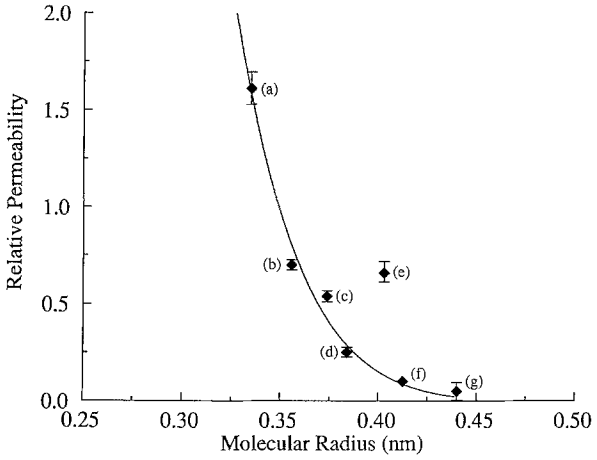

Fig. 4. The relation between the permeability (relative to Na^+) and molecular radius for the monovalent organic cations listed in Table 3. The Stokes-Einstein radius (r_{se}) was calculated from the limiting conductivities (λ) of the ions with the formula: $r_{se} \cdot \lambda$ = constant [30], the constant being determined from the behavior of tetraethylammonium at 25°C, for which λ = 44.9 $cm^2\ \Omega^{-1}$, $equiv^{-1}$, and r_{se} = 0.204 nm. The Stokes-Einstein radius was then converted to the molecular radius using correction factors read off from Figure 6.1 in Robinson and Stokes [30]. The equivalent limiting conductance for ethanolamine is given in Robinson and Stokes [30] and those of the other ions were calculated from their molecular weights by the formula, $MW^{0.5} \cdot \lambda$ = constant [30], the constant being determined by the values for ethanolamine at 25°C: MW = 62.1 and λ = 4.42 $cm^2\ \Omega^{-1}\ equiv^{-1}$. The cations are (*a*) guanidinium, (*b*) ethanolamine, (*c*) diethylamine, (*d*) piperazine, (*e*) 4-aminopyridine, (*f*) Tris and (*g*) N-methylglucamine. The solid line is a least-squares fit of the Renkin equation to the relative permeabilities for the organic cations other than 4-aminopyridine (*e*). Each point is the mean of three or four experiments ± SEM

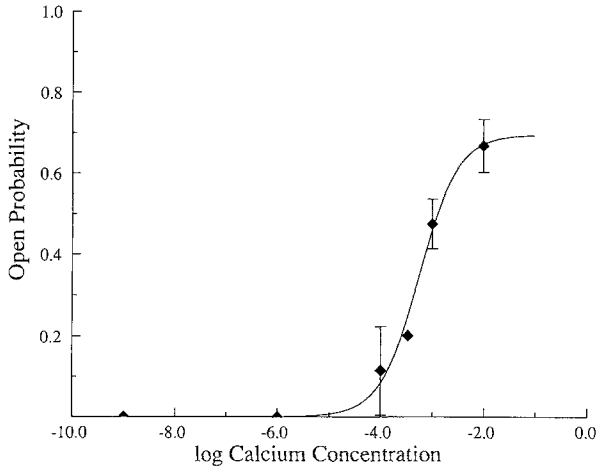

Fig. 5. The relation between open probability and cytosolic Ca^{2+} concentration in excised inside-out patches. The unbroken line is a least-squares fit of the Hill equation. Each point is the mean of three experiments ± SEM, with the exception of the point at 3 × 10^{-4} mol/liter Ca^{2+} which is from a single experiment. For those patches in which multiple channels were active, we calculated open probabilities by assuming that the number of channels open at any instant is described by a binomial distribution and that the number of channels present in the patch is equal to the maximum number open during the time in which the record was made

liter Ca^{2+} in the bathing solution (Fig. 6). In each case, the results were obtained from at least four inside-out patches, all of which had a greater than 99% probability than they contained only one active channel, determined as outlined in Eqs. (6) and (7). The channel was clearly activated by depolarization of the cell membrane. The open probability at −60 mV was 79% which declined to 28% when the holding potential was increased to +60 mV.

Kinetic analysis of recordings from outside-out patches held at +60 mV in which only one channel appeared to be active showed that the open-time histogram could best be described by two exponentials (Fig. 7*A*) with time constants of 1.0 and 11.4 msec. The closed-time histogram also required two exponentials to fit it (Fig. 7*B*), with time constants of 1.0 and 20.0 msec. Figure 7 also shows the open- and closed-time histograms for the channel when it was held at −60 mV. Once again, the open-time histogram could be described by two exponentials (with time constants of 1.3 and 9.2 msec), as could

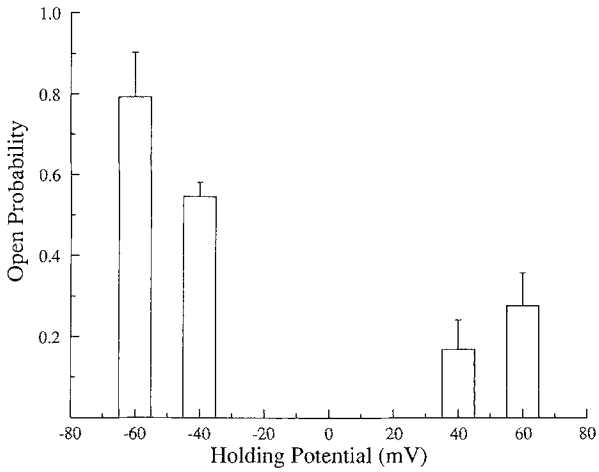

Fig. 6. The effect of pipette holding potential on the open probability of the 25-pS nonselective channel in inside-out excised patches. The height of each bar is the average from four inside-out patches ± SEM. The patches used in preparing this figure had a greater than 99% probability of having only a single channel active (*see* Materials and Methods)

the closed-time histogram (with time constants of 9.2 and 43 msec). The channel thus had at least two open and two closed states. The time constants describing the open-time distribution were little influenced by the transmembrane potential, but the slow time constant describing the distribution of closed times was markedly reduced as the patch was de-

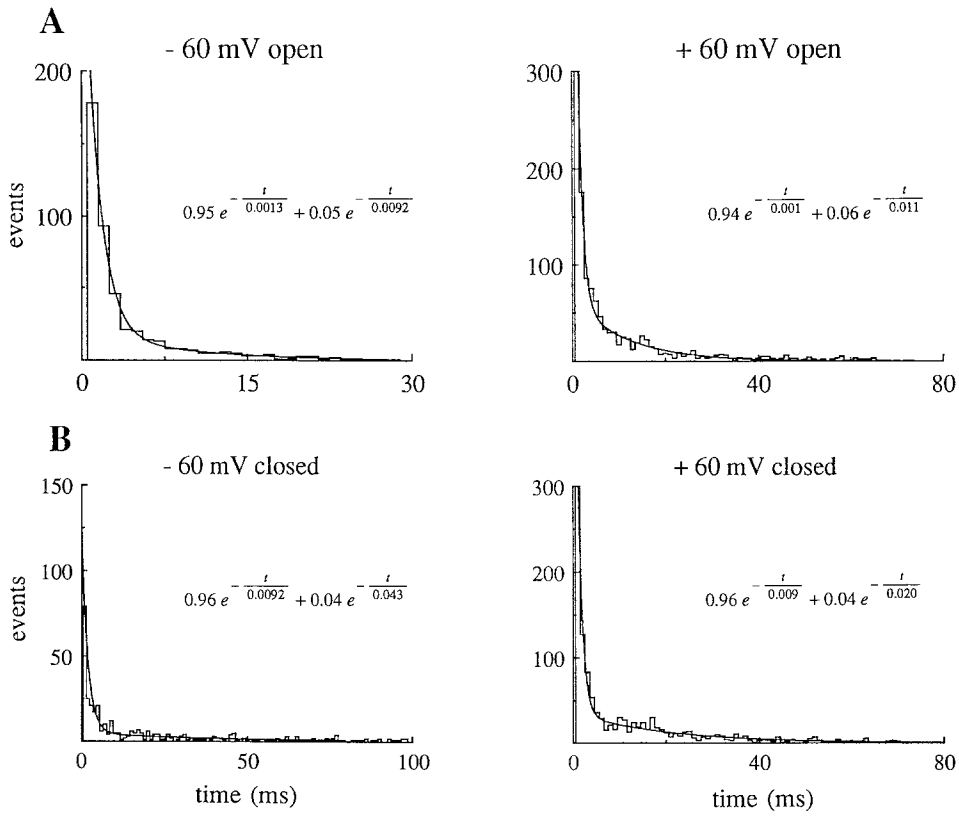

Fig. 7. (*A*) Open-time and (*B*) closed-time histograms for the 25-pS nonselective cation channel in an inside-out patch held at pipette potentials of +60 and −60 mV. The curves are least-squares fits of two exponentials to the dwell-time histogram data. The parameters of the fitted equations are given in each panel. The parameter t is the dwell time in seconds. The patch used in this figure had a greater than 99% probability of having only a single channel active (*see* Materials and Methods)

polarized. The activation of the nonselective channel by depolarization thus appeared to be due to destabilization of the closed states rather than to stabilization of the open states.

The channel was blocked by the addition of 0.1 mmol/liter AMP to the cytosolic surface (Fig. 8) and also by ATP (0.1 mmol/liter) (*results not shown*). We also found that the channel was blocked by diphenylamine-2-carboxylate (DPC, 0.1 mmol/liter) (Fig. 9) when this compound was added to the extracellular surface. The single-channel records (Fig. 9*B*) indicate that DPC in this concentration produces an almost complete blockade of the 25-pS channel. The current histogram (Fig. 9*A*), which showed a marked reduction in currents through the patch in the presence of DPC, confirms that the absence of single-channel transitions in the tracing in Fig. 9*B* is due to channel blockade. This block was not influenced by transmembrane voltage, and from the occasional openings that we observed in the presence of DPC, it would appear that the blockade was of the "slow" type (*data not shown*).

Quinine (0.1 mmol/liter), when added to the cytosolic surface of an excised inside-out patch, produced a rapid "intermediate" blockade that was strongly voltage dependent, being most pronounced when the patch was depolarized (Fig. 10*A*) by making the pipette potential negative with respect to the bath. When added to the outside surface of an excised outside-out patch, quinine (0.1 mmol/liter) also produced a voltage-dependent "intermediate" type of blockade (Fig. 10*B*), which, as in inside-out patches, was most pronounced when the patch was depolarized (i.e., when the pipette was made positive with respect to the bath). Thus, quinine blockade from either side of the channel was enhanced by depolarization. The basis for this surprising behavior is discussed below.

Surprisingly, 4-aminopyridine, which permeated when present on the extracellular surface of the channel, caused a "slow" type of blockade when present in a concentration of 1 or 5 mmol/liter on the cytosolic side of inside-out excised patches (Fig. 11*A*). This blockade was not voltage dependent and was characterized by prolonged closures and a reduction in the number of active channels. Exposure of the extracellular surface to up to 130

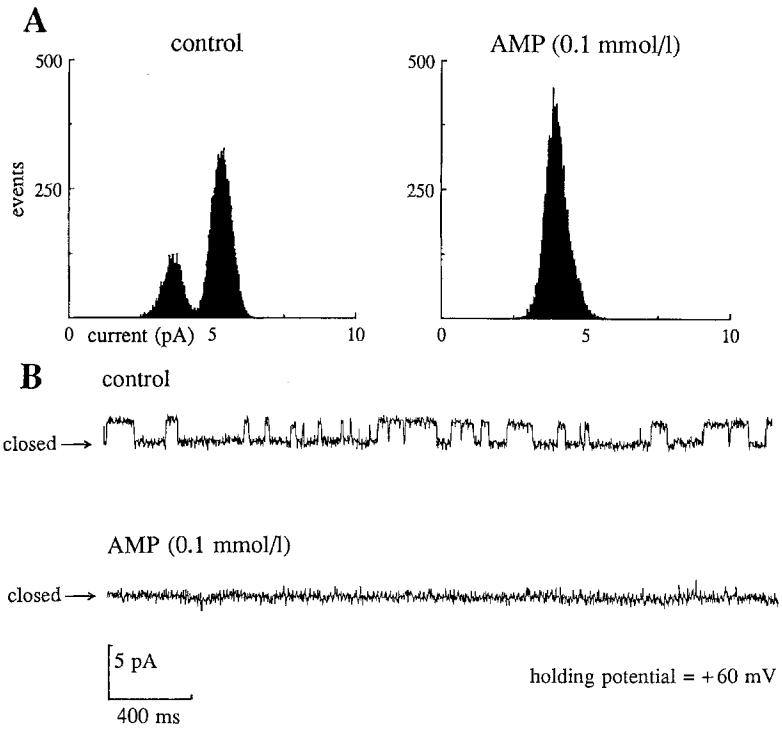

Fig. 8. The effect of the addition of 0.1 mmol/liter AMP to the cytosolic surface of an excised inside-out patch at pipette potential of +60 mV. (*A*) Histograms of the current flowing through the patch at 1-msec intervals during 20-sec recordings taken before and after the addition of the blocker. (*B*) Representative single-channel recordings before and after the addition of AMP to the bath

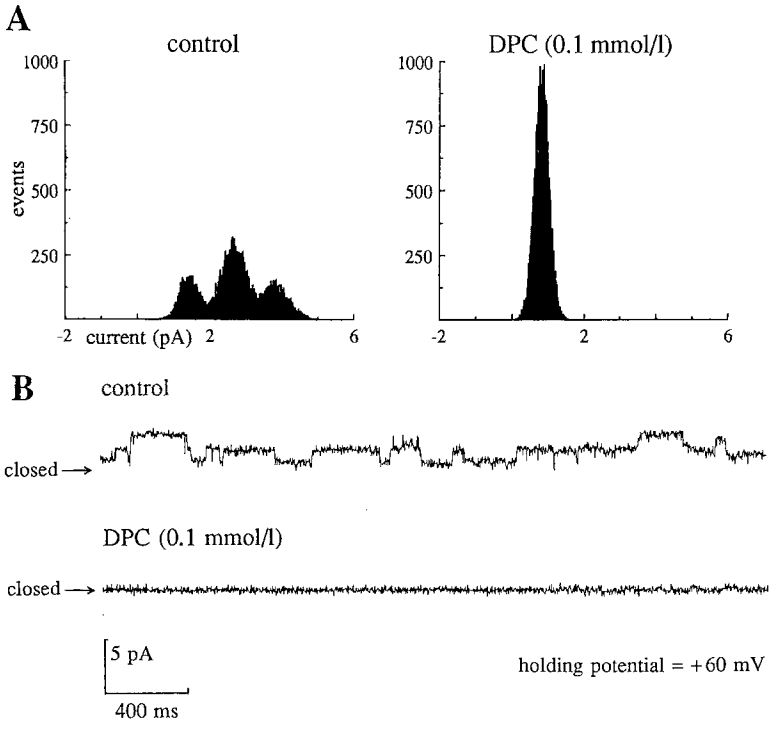

Fig. 9. The effect of the addition of diphenylamine-2-carboxylic acid (DPC; 0.1 mmol/liter) to the extracellular surface of an excised outside-out patch held at a pipette potential of +60 mV. (*A*) Hitograms of the current flowing through the patch at 1-msec intervals during 20-sec recordings taken before and after the addition of the blocker. (*B*) Representative single-channel recordings before and after the addition of DPC to the bath

mmol/liter 4-aminopyridine failed to block the channel at all (Fig. 11*B*). Indeed, as shown above (Table 3 and Fig. 3) 4-aminopyridine can actually permeate the nonselective cation channel when present on the extracellular surface.

SITS (0.1 mmol/liter), when added to the cytosolic surface of the patch, also led to single-channel recordings characterized by the absence of single-channel activity (Fig. 12*B*). As the current histogram in Fig. 12*A* makes clear, however, this was

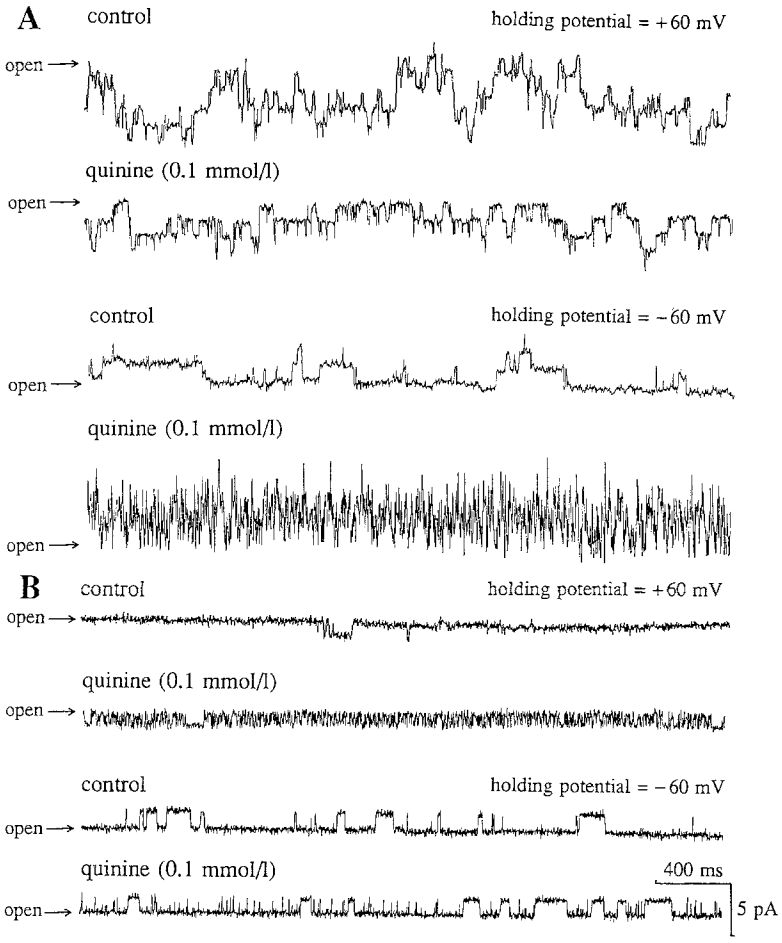

Fig. 10. (*A*) Single-channel record from an excised inside-out patch showing the effect of 0.1 mmol/liter quinine added to the cytosolic surface when the pipette potential was +60 mV and when it was −60 mV. Quinine produced a rapid flickering block that was most noticeable at −60 mV. (*B*) Single-channel record showing the effect of 0.1 mmol/liter quinine added to the extracellular surface of an excised outside-out patch when the pipette potential was +60 mV and when it was −60 mV. Quinine produced a rapid flickering block that was most noticeable at +60 mV

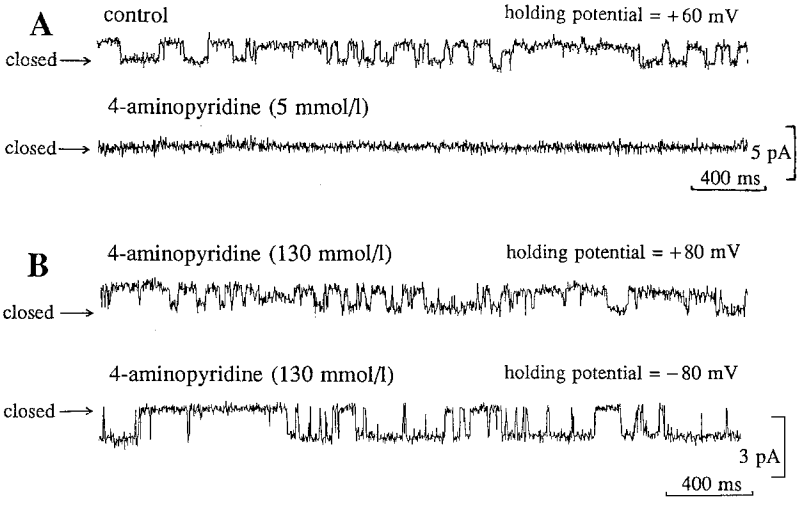

Fig. 11. Single-channel records showing the effects of 4-aminopyridine on the nonselective cation channel. (*A*) Single-channel records showing the nonselective cation channel in an excised inside-out patch at a pipette potential of +60 mV before and after the addition of 4-aminopyridine (5 mmol/liter) to the bath. (*B*) Single-channel records showing that the presence of 130 mmol/liter 4-aminopyridine and 30 mmol/liter Na^+ in the pipette did not inhibit channel activity at either hyperpolarized or depolarized pipette potentials

due to irreversible channel activation, not channel blockade. The occasional transitions that occurred following the addition of SITS (Fig. 10*B*) were of the same size as those seen prior to the addition of SITS, which indicates that SITS was increasing the channel open probability rather than the single-channel current. Quinine (0.1 mmol/liter), which as described above, produces an "intermediate" blockade when added to the cytosolic surface of inside-out patches, produced the flickering charac-

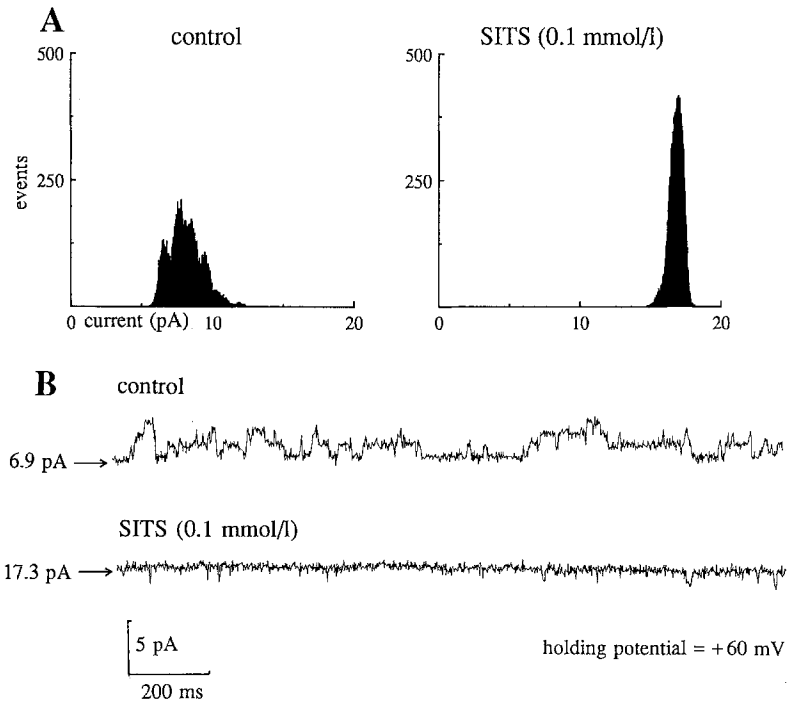

Fig. 12. Effect of the addition of 0.1 mmol/liter SITS to the intracellular surface of an excised inside-out patch held at a pipette potential of +60 mV. (*A*) Histograms of the current flowing through the patch at 1-msec intervals taken before and after the addition of the drug. (*B*) Representative single-channel recordings before and after treatment with SITS

teristic of this type of blockade and reduced the current flowing through the patch when it was added to a patch previously exposed to SITS, thereby confirming that SITS was holding the channels open. The ability of AMP to close channels held open by SITS was not impaired (*data not shown*).

We exploited the ability of SITS to lock the nonselective cation channel into an open state in order to study the kinetics of quinine blockade. When quinine (100 μmol/liter) was added to the cytosolic side of a patch already exposed to SITS, we found that the distributions of the open times and blocked times could be described by single exponentials and the voltage dependence of the time constants indicated that the quinine binding site sensed 60% of the transmembrane voltage (*data not shown*).

Discussion

We report here the characteristics of the 25-pS nonselective cation channel as expressed in the cultured salivary cell line ST_{885}. Many of its properties are similar to those found in the nonselective cation channels described in other exocrine tissues: cultured sweat gland cells [14], pancreatic acini [11, 21], pancreatic ducts [12], lacrimal end-pieces [16] and thyroid follicles [18].

Ca^{2+} and Voltage Sensitivity

As pointed out in the Introduction, the 25-pS nonselective cation channels that have been described so far in the literature are heterogeneous with respect to the sensitivity of their open probabilities to transmembrane voltage and to the level of cytosolic Ca^{2+}. The channel in ST_{885} cells is activated by depolarization, and in inside-out patches it requires Ca^{2+} concentrations in excess of 10^{-4} mol/liter to activate it. The Ca^{2+} dose-response curve actually shows that a high Ca^{2+} concentration alone is not sufficient to open the channel fully since the dose-response curve reached a plateau at an open probability of 67% (when the Ca^{2+} concentration was 10^{-2} mol/liter). Further increases in Ca^{2+} concentration actually reduced the open probability but we do not have sufficient information to decide whether this was due to Ca^{2+} blocking the pore or to the high Ca^{2+} concentration causing formation of ineffective Ca^{2+}-channel complexes (i.e., competitive self-inhibition of Ca^{2+} activation as a result of the high ambient Ca^{2+} concentration).

In its Ca^{2+} and voltage sensitivity properties, the nonselective cation channel in ST_{885} cells is similar to the channels found by Sturgess et al. [35] in rat insulinoma cells, and by Bevan et al. [3] in Schwann cells, and to the 28-pS channel observed by Ehara et al. [10] in ventricular myocytes. In some of the other exocrine tissues in which this channel type

has been reported, the open probability was not voltage sensitive and the channel was activated by Ca^{2+} concentrations only in the micromolar range: mouse pancreatic acini [19], rat and mouse salivary endpiece cells [17], rat thyroid follicular cells [18] and guinea pig pancreatic acinar cells [36]. The observation that the Ca^{2+}-sensitivity of the channel in excised patches from pancreatic acinar cells declines rapidly after excision, and that the channel can be activated by Ca^{2+} concentrations as low as 5×10^{-7} mol/liter when studied in cell-attached patches on saponin-permeabilized cells [21], suggests very strongly that the Ca^{2+} sensitivity of the mouse pancreatic channel must have been enhanced by the presence of some intracellular substance that was too large to diffuse rapidly out of the permeabilized cell. Although we have not observed any change in the Ca^{2+} sensitivity of the channel in ST_{885} cells following patch excision, our finding that the nonselective cation channel is active in cell-attached patches does support the idea that the channel is activated by an intracellular substance. If the difference in Ca^{2+} sensitivity is to be attributed to different conformations of a single protein, then the shift in conformation must have been very great because the transition from high sensitivity to low sensitivity forms was accompanied by the development of voltage sensitivity.

Blockers and Activators

The studies with channel blockers and activators suggest that the Ca^{2+}-activated nonselective cation channel in ST_{885} cells must be similar to those with higher Ca^{2+} sensitivities found in other exocrine tissues. Thus, ATP has been found to block the nonselective cation channel in guinea pig pancreatic acinar cells [36] and the channel is blocked by DPC and activated by SITS applied from the cytosolic surface in rat pancreatic acinar cells [11]. It is surprising to note that although DPC blocked the nonselective cation channel in both pancreatic and mandibular secretory cells of the rat, it did so from opposite surfaces of the plasma membrane, cytosolic in the pancreas [11] and the external surface in the mandibular gland (present studies). Needless to say, in the light of the findings in the pancreas [11], we rechecked our findings by repeating the experiments; we also tested DPC from the cytosolic surface and found it to be without effect. We have no explanation for the difference. The sensitivity of the nonselective cation channel in ST_{885} cells to AMP, ATP, quinine and to 4-aminopyridine, also links it closely to another nonselective cation channel with a low sensitivity to Ca^{2+}, that found in rat insulinoma cells [35].

The findings with quinine are of particular interest. We found that quinine causes a block of intermediate type from both the cytosolic and the extracellular sides of the nonselective cation channel. Yet from either side, depolarization of the patch caused the effectiveness of the block to increase. It is not surprising that depolarization of the patch should enhance the effectiveness of cytosolic quinine, because if the quinine binding site senses part of the transmembrane potential, depolarization should increase the amount of quinine bound, but it was very surprising to observe that depolarization also enhanced the effectiveness of extracellular quinine, because depolarization under these circumstances should decrease the amount of quinine bound. Clearly these observations are not compatible with a simple model in which extracellular quinine enters the channel pore and blocks it. We have two explanations for voltage dependency of the quinine block. The first is that quinine only blocks from the cytosolic surface of the channel, and that extracellular quinine acts by diffusing through the membrane and entering the channel from the cytosolic side. The second possibility is that extracellular quinine is blocking by binding to a conformation of the channel protein that is stabilized by depolarization. In this model, the binding site for extracellular quinine might not even be within the channel pore or sense any fraction of the transmembrane potential. We do not currently have any evidence that would permit us to distinguish between these alternative explanations.

Channel Kinetics

Analysis of the channel kinetics also shows many similarities with nonselective channels having a high affinity for Ca^{2+}. In ST_{885} cells, the open- and closed-time distributions are both described by two exponentials but only the slow time constant describing the closed-time distribution is voltage dependent. It becomes faster as the membrane is depolarized, so causing an increase in channel open probability with depolarization. The kinetics suggest the presence of at least two open and two closed states, a complex mechanism similar to that observed by Sturgess et al. [35] in rat insulinoma cells and Siemen and Reuhl [33] in brown adipose cells.

Ion Permeability: Similarities to the Nicotinic ACh Receptor Channel

Our studies on the relative permeabilities of the channel to inorganic and organic cations have revealed some striking similarities to the endplate

ACh receptor channel. With the exception that Rb^+ was swapped with Li^+, the relative permeabilities to inorganic cations that we have found (*see* Table 2) are the same as those reported for the frog endplate channel, *viz.*, NH_4^+ (1.79) > Rb^+ (1.30) > K^+ (1.11) > Na^+ (1.0) > Li^+ (0.87) [1, 9]. The transposition of Rb^+ with Li^+ suggests that the nonselective cation channel cannot be regarded simply as a watery pore, an impression that is strengthened when we look at the data obtained on the permeation of organic cations (Table 3). Once again the similarities with findings in the frog endplate channel, *viz.*, NH_4^+ (1.79) > guanidinium (1.59) > Na^+ (1.0) > ethanolamine (0.72) > 4-aminopyridine (0.54) > diethylamine (0.38) > piperazine (0.30) > Tris (0.18) > N-methylglucamine (0.034) [9], are striking, the ST_{885} nonselective cation channel showing an identical rank order of permeabilities (Table 3). When we fitted the Renkin equation [29] to our data we found that the ST_{885} channel behaved like a cylinder with a radius of 0.49 nm, which is similar to the radius of the ACh receptor channel determined by Dwyer et al. [9], *viz.*, 0.37 nm. (The small difference arises largely because Dwyer et al. [9] attempted to exclude the effect of the hydration shell when assessing molecular radius whereas we have included it.) In both the endplate ACh receptor channel and the nonselective cation channel, the permeation of 4-aminopyridine was anomalous (*compare* Fig. 2 of this paper with Fig. 5 of Dwyer et al. [9]), its relative permeability being considerably higher than would be expected on the basis of its molecular radius. Furthermore, in both channels the compound acts as a blocker and yet is quite permeant when present in high concentrations. In endplate ACh receptor channels, the ability of large, permeable cations to act as blockers has been explained by Sanchez et al. [32] as being due to their interaction with a binding site within the channel for which they have a high affinity. In contrast to the case with the endplate channel [32], 4-aminopyridine blockade of the ST_{885} channel was not influenced by transmembrane potential. We conclude from this that the binding site for 4-aminopyridine in the nonselective cation channel must be in a position where it does not sense a significant part of the transmembrane potential. Another finding of interest was that Tris and N-methylglucamine, which are widely used as "impermeant" substitutes for common inorganic cations, have measurable permeabilities through the nonselective cation channel. Tris has also been found to permeate the nonselective cation channel in the bursting cells of *Helix* [24].

We also measured the permeabilities of Mg^{2+} and Ca^{2+} relative to Na^+ and found that, as in the endplate ACh receptor channel, Mg^{2+} is slightly permeant (about 7% as permeant as Na^+). Unlike the endplate channel, however, where Ca^{2+} exhibits between 10 and 20% of the permeability of Na^+, we were unable to demonstrate any permeability to Ca^{2+} in the ST_{885} channel. Since it is known that there is an inverse relation between the ambient Ca^{2+} concentration and the Ca^{2+} permeability of the endplate channel [1], we repeated our measurements in ST_{885} cells with only 20 mmol/liter Ca^{2+} in the pipette solution, but we were still unable to demonstrate any permeability to Ca^{2+}. We have not taken into account the effects of membrane surface charge in these estimates of divalent cation permeability but, since surface charge does not alter the reversal potential of an ion channel that is permeable only to monovalent cations [2, 37], our finding that Ca^{2+} does not permeate the nonselective cation channel in ST_{885} cells would not be altered by the inclusion of such effects. In the case of Mg^{2+}, which does appear to be permeable, our neglect of surface charge will have led to overestimation of the permeability of Mg^{2+} relative to Na^+ but the extent of this overestimation is not known because we do not have any measurements of the surface charge on these cells. Nevertheless, a simple example will show its possible magnitude. If we assume a surface charge of 10^{-5} C cm^{-2}, which is in the middle of the range measured for the extracellular surface of nerve and muscle membranes [2, 37], we find that a reversal potential of +43 mV indicates a permeability to Mg^{2+} relative to Na^+ of as little as 0.005, which is 10 times lower than that we have estimated when ignoring surface change. Consequently, our estimate of the relative permeability of Mg^{2+} may be a substantial overestimate. Although it remains possible that very small amounts of Ca^{2+} do enter exocrine cells through these channels [21], we believe that their low Ca^{2+} permeability makes it unlikely that they could represent an important pathway for Ca^{2+} entry to the cell.

The Role of the Nonselective Cation Channel in Secretion

What then is the role of the nonselective cation channels in secretory epithelia? As mentioned in the Introduction, regardless of whether the channel is in the apical or the basolateral membrane, it would inhibit secretion in any epithelium relying on the classical model as proposed by Silva et al. [34] for the shark rectal gland. This is because the drive for Cl^- secretion in Silva's model is due to the cell membrane potential being lower than the Nernst potential for Cl^-, so that nonselective cation channels,

by depolarizing the cell, would be expected to reduce this drive. This suggests that in epithelia where the channel appears to be active during secretion (mouse pancreas, rat lacrimal gland, rat pancreatic ducts), the process must be driven by a mechanism that is either insensitive to membrane voltage or is stimulated by depolarization. In considering the role of the channel it should also be remembered that in at least one epithelium, *viz.*, rat pancreatic duct [12], it is found both in apical and basolateral membranes. Indeed, this might well be the rule rather than the exception because in most of the epithelia that have so far been studied by patch-clamp methods, only one or the other membrane has been readily accessible to investigation (i.e., the apical membrane in cultured epithelia, and the basolateral membrane in tissue fragments and dispersed cells).

It is quite possible to devise models for epithelial secretion in which the presence of nonselective cation channels in the plasma membrane would be advantageous. An extreme example would be an epithelium in which secretion was due to the movement of K^+ across the apical membrane into the lumen with change balance being maintained by the movement of Cl^- through the tight junctions and Na^+ through nonselective cation channels in the basolateral membrane (i.e., a reversed epithelial current loop model). The K^+ would then have to exchange with Na^+ through the tight junctions so as to give rise to a Na^+-rich secretion. In such a mechanism, only two Cl^- ions would be secreted per molecule of ATP hydrolyzed, which is only one-third as efficient as a secretory process driven by Na^+-K^+-$2Cl^-$ cotransport. For tissues in which the bulk of the Na^+ entering the cell is not carried by a Na^+-K^+-$2Cl^-$ cotransporter, however, but via a Na^+-H^+ exchanger or a Na^+-amino acid cotransporter, it could be a satisfactory alternative secretion mechanism.

It is also possible to conceive of hybrid models in which both K^+-driven and Cl^--driven secretion occur simultaneously. Indeed, these can be more efficient [8] than the standard current loop model. If, for example, the apical membrane contained both K^+ and Cl^- channels, and the basolateral membrane had a sufficiently high K^+ conductance to keep the cell potential away from the Nernst potential for Cl^-, then the epithelium would secrete both K^+ and Cl^- into the lumen across the apical membrane and the secreted fluid would become Na^+ rich as a result of exchange of K^+ for Na^+ across the tight junctions. Secretion by this mechanism would not depend exclusively on a current loop and so would not necessarily be adversely affected by the presence of nonselective cation channels in the basolateral membrane. The presence of a Na^+ leak across the basolateral membrane might even be helpful because it would cause the Na^+-,K^+-ATPase to pump additional K^+ into the cytosol which could then be secreted across the apical membrane. The role of apical nonselective cation channels, as seen in the rat pancreatic ducts [12], remains a mystery however. It is difficult to see how they could ever support secretion.

This project was supported by the National Health and Medical Research Council of Australia. We thank Dr. H. Gögelein for his valuable discussion of the data and Professor R. Greger for the gift of DPC and other chloride channel blockers.

References

1. Adams, D.J., Dwyer, T.M., Hille, B. 1980. The permeability of endplate channels to monovalent and divalent metal cations. *J. Gen. Physiol.* **75**:493–510
2. Barry, P.H., Gage, P.W. 1984. Ionic selectivity of channels at the end plate. *In:* Ion Channels: Molecular and Physiological Aspects *Curr. Topics Membr. Transport* **21**:1–51
3. Bevan, S., Gray, P.T.A., Ritchie, J.M. 1984. A calcium-activated cation-selective channel in rat cultured Schwann cells. *Proc. R. Soc. Lond. [Biol.]* **222**:349–355
4. Bezanilla, F. 1985. A high capacity data recording device based on a digital audio processor and a video cassette recorder. *Biophys. J.* **47**:437–441
5. Colquhoun, D., Hawkes, A.G. 1983. The principles of the stochastic interpretation of ion-channel mechanisms. *In:* Single-Channel Recording. B. Sakmann and E. Neher, editors. pp. 135–175. Plenum, New York
6. Colquhoun, D., Neher, E., Reuter, H., Stevens, C.F. 1981. Inward current channels activated by intracellular Ca in cultured cardiac cells. *Nature (London)* **294**:752–754
7. Cook, D.I., Towner, S.P., Young, J.A. 1986. Patch-clamp studies of cultured salivary cells. *Biomed. Res.* **7 (Suppl. 2)**:203–207
8. Cook, D.I., Young, J.A. 1989. The effect of K^+ channels in the apical plasma membrane on epithelial secretion based on secondary active Cl^- transport. *J. Membrane Biol.* **110**:139–146
9. Dwyer, T.M., Adams, D.J., Hille, B. 1980. The permeability of the endplate channel to organic cations in frog muscle. *J. Gen. Physiol.* **75**:469–492
10. Ehara, T., Noma, A., Ono, K. 1988. Calcium-activated nonselective cation channel in ventricular cells isolated from adult guinea-pig hearts. *J. Physiol. (London)* **403**:117–134
11. Gögelein, H., Pfannmüller, B. 1988. The nonselective cation channel in the basolateral membrane of rat exocrine pancreas. Inhibition by 3',5-dichlorodiphenylamine-2-carboxylic acid (DCDPC). *Pfluegers Arch.* **413**:287–298
12. Gray, M.A., Greenwell, J.R., Argent, B.E. 1988. Ion channels in pancreatic duct cells and their role in bicarbonate secretion. *In:* Exocrine Secretion. P.Y.D. Wong and J.A. Young, editors. pp. 77–80. Hong Kong University Press, Hong Kong
13. Hamill, O.P., Marty, A., Neher, E., Sakmann, B., Sigworth, F.S. 1981. Improved patch-clamp techniques for high resolution current recording from cells and cell free membrane patches. *Pfluegers Arch.* **391**:85–100

14. Krouse, M.E., Hagiwara, G., Chen, J., Lewiston, N.L., Wine, J.J. 1988. Ion channels in normal and cystic fibrosis cultured sweat gland cells. *In:* Exocrine Secretion. P.Y.D. Wong and J.A. Young, editors. pp. 99–102. Hong Kong University Press, Hong Kong
15. Martin, D.K., Cook, D.I., Young, J.A. 1989. A direct-reading device for measurement of micropipette diameters. *Proc. Aust. Physiol. Pharmacol. Soc.* **20:**171P
16. Marty, A., Tan, Y.P., Trautmann, A. 1984. Three types of calcium-dependent channels in rat lacrimal glands. *J. Physiol. (London)* **357:**293–325
17. Maruyama, Y., Gallacher, D.V., Petersen, O.H. 1983. Voltage and Ca^{2+}-activated K^+ channel in basolateral acinar cell membranes in mammalian salivary glands. *Nature (London)* **302:**827–829
18. Maruyama, Y., Moore, D., Petersen, O.H. 1985. Calcium-activated cation channel in rat thyroid follicular cells. *Biochim. Biophys. Acta* **821:**229–232
19. Maruyama, Y., Petersen, O.H. 1982. Cholecystokinin activation of single-channel currents is mediated by an internal messenger in pancreatic acinar cells. *Nature (London)* **300:**61–63
20. Maruyama, Y., Peterson, O.H. 1982. Single-channel currents in isolated patches of plasma membrane from basal surface of pancreatic acini. *Nature (London)* **299:**159–161
21. Maruyama, Y., Petersen, O.H. 1984. Single calcium-dependent cation channels in mouse pancreatic acinar cells. *J. Membrane Biol.* **81:**83–87
22. Mittman, S., Flaming, D.G., Copenhagen, D.R., Belgum, J.H. 1987. Bubble pressure measurement of micropipette tip outer diameter. *J. Neurosci. Methods* **22:**161–166
23. Neter, J., Wasserman, W. 1974. Applied Linear Statistical Models. Regression, Analysis of Variance, and Experimental Designs. Richard D. Irwin, Homewood (IL)
24. Partridge, L.D., Swandulla, D. 1987. Single Ca-activated cation channels in bursting neurone of *Helix*. *Pfluegers Arch.* **410:**627–631
25. Partridge, L.D., Swandulla, D. 1988. Calcium-activated non-specific cation channels. *Trends Neurosci.* **11:**69–72
26. Petersen, O.H., Maruyama, Y. 1983. What is the mechanism of the calcium influx to pancreatic acinar cells evoked by secretagogues. *Pfluegers Arch.* **396:**82–84
27. Petersen, O.H., Maruyama, Y. 1984. Calcium-activated potassium channels and their role in secretion. *Nature (London)* **307:**693–696
28. Poronnik, P., Cook, D.I., Young, J.A. 1988. The use of Cytodex® microcarrier beads in patch-clamp studies on cultured epithelial cells. *Pfluegers Arch.* **413:**90–92
29. Renkin, E.M., Curry, F.E. 1979. Transport of water and solutes across capillary endothelium. *In:* Membrane Transport in Biology. G. Giebisch, editor. Vol. IVA (Transport Organs). pp. 1–45. Springer-Verlag, Berlin
30. Robinson, R.A., Stokes, R.H. 1965. Electrolyte Solutions. (2nd Ed.) Butterworths, London
31. Sachs, F., Neil, J., Barkakati, N. 1982. The automated analysis of data from single ionic channels. *Pfluegers Arch.* **395:**331–340
32. Sanchez, J.G., Dani, J.A., Siemen, D., Hille, B. 1986. Slow permeation of organic cations in acetylcholine receptor channels. *J. Gen. Physiol.* **87:**985–1001
33. Siemen, D., Reuhl, T. 1987. Non-selective cationic channel in primary cultured cells of brown adipose tissue. *Pfluegers Arch.* **408:**534–536
34. Silva, P., Stoff, J., Field, M., Fine, L., Forrest, J.N., Epstein, F.J. 1977. Mechanism of active chloride secretion by shark rectal gland: Role of Na-K-ATPase in chloride transport. *Am. J. Physiol.* **233:**F298–F306
35. Sturgess, N.C., Hales, C.N., Ashford, M.L.J. 1987. Calcium and ATP regulate the activity of a non-selective cation channel in a rat insuljnoma cell line. *Pfluegers Arch.* **409:**607–615
36. Suzuki, K., Petersen, O.H. 1988. Patch-clamp study of single channel and whole cell K^+ currents in guinea pig pancreatic acinar cells. *Am. J. Physiol.* **255:**G275–G285
37. Takeda, K., Gage, P.W., Barry, P.H. 1982. Effects of divalent cations on toad end-plate channels. *J. Membrane Biol.* **64:**55–66
38. Von Tscharner, V., Prod'hom, B., Baggiolini, B., Reuter, H. 1986. Ion channels in human neutrophils activated by a rise in cytosolic calcium concentration. *Nature (London)* **324:**369–372
39. Yellen, G. 1982. Single Ca^{2+}-activated nonselective cation channels in neuroblastoma. *Nature (London)* **296:**357–359
40. Young, J.A., Cook, D.I., Van Lennep, E.W., Roberts, M.L. 1987. Secretion by the major salivary glands. *In:* Physiology of the Gastrointestinal Tract. (2nd Ed.) L. Johnson, J. Christensen, M. Jackson, E. Jacobson, and J. Walsh, editors. Vol. 2, pp. 773–815. Raven, New York

Received 22 June 1989; revised 16 October 1989